Global Energy Interconnection
Development and Cooperation Organization

ELSEVIER
Production And Hosting By Elsevier On Behalf Of KeAi
KeAi

Volume 7 Number 5 October 2024 682-696
DOI: 10.1016/j.gloei.2024.10.009
Global Energy Interconnection
Contents lists available at ScienceDirect
https: //www.sciencedirect.com/journal/global-energy-interconnection

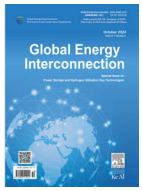

Optimizing PID controller parameters for robust automatic voltage regulator system through indirect design approach-2

Mohd Zaidi Mohd Tumari[1], Mohd Ashraf Ahmad[2], Mohd Riduwan Ghazali[2], Mohd Helmi Suid[2]

1. Faculty of Electrical Technology and Engineering, Universiti Teknikal Malaysia Melaka, Durian Tunggal, 76100, Malaysia
2. Faculty of Electrical and Electronics Engineering Technology, Universiti Malaysia Pahang Al Sultan Abdullah, Pekan, 26600, Malaysia

Scan for more details

Abstract: Automatic voltage regulators (AVR) are designed to manipulate a synchronous generator's voltage level automatically. Proportional integral derivative (PID) controllers are typically used in AVR systems to regulate voltage. Although advanced PID tuning methods have been proposed, the actual voltage response differs from the theoretical predictions due to modeling errors and system uncertainties. This requires continuous fine tuning of the PID parameters. However, manual adjustment of these parameters can compromise the stability and robustness of the AVR system. This study focuses on the online self-tuning of PID controllers called indirect design approach-2 (IDA-2) in AVR systems while preserving robustness. In particular, we indirectly tune the PID controller by shifting the frequency response. The new PID parameters depend on the frequency-shifting constant and the previously optimized PID parameters. Adjusting the frequency-shifting constant modifies all the PID parameters simultaneously, thereby improving the control performance and robustness. We evaluate the robustness of the proposed online PID tuning method by comparing the gain margins (GMs) and phase margins (PMs) with previously optimized PID parameters during parameter uncertainties. The proposed method is further evaluated in terms of disturbance rejection, measurement noise, and frequency response analysis during parameter uncertainty calculations against existing methods. Simulations show that the proposed method significantly improves the robustness of the controller in the AVR system. In summary, online self-tuning enables automated PID parameter adjustment in an AVR system, while maintaining stability and robustness.

Keywords: PID controller tuning; AVR system; Indirect design approach (IDA); Frequency-shifting; Robust control

0 Introduction

Synchronous generators are the most widely used equipment for power generation owing to their ability to produce electricity across a broad operating range. The terminal voltages of these synchronous generators can be regulated to a set-point value under fluctuating

Received: 28 April 2024/ Revised: 16 June 2024/ Accepted: 20 August 2024/ Published: 25 October 2024

✉ Mohd Ashraf Ahmad
mashraf@umpsa.edu.my

Mohd Riduwan Ghazali
riduwan@umpsa.edu.my

Mohd Zaidi Mohd Tumari
mohdzaidi.tumari@utem.edu.my

Mohd Helmi Suid
mhelmi@umpsa.edu.my

load conditions by controlling the exciter input voltage. Maintaining a steady terminal voltage is critical in power system networks because the proper functioning and reliability of connected electrical devices depend on preserving the nominal system voltage. Therefore, the primary goal of control in power systems is to stabilize the voltage magnitude at a consistent nominal level. By preventing the voltage from deviating, the sensitive equipment can continue to operate as intended. Effective voltage control enables the integration of synchronous generators across expansive and variable power grids [1]. Employing an automatic voltage regulator (AVR) enables the generator's output voltage to be maintained at the set point. This improves the stability, reliability, and power quality of the power system amid voltage fluctuations. However, achieving rapid and stable AVR control is challenging due to load variations and high inductance in the alternator field coils. Hence, enhancing the control performance of AVR systems is critical for ensuring stable and reliable power distribution across the grid. Therefore, research efforts continue to focus on advancing voltage-control responsiveness and transient stability to augment power-system distribution capabilities.

A considerable amount of literature has been published on the development of accurate controllers for AVR systems. These studies include fuzzy logic controllers (FLCs) [2], sliding mode controllers [3], adaptive neuro-fuzzy inference systems [4], and brain emotional learning-based intelligent controllers [5]. In recent decades, proportional-integral-derivative (PID) controllers have become the most widely used controllers in research. PID controllers offer robust performance, a simple structure, and low computational demand [6]. Therefore, they have been extensively utilized across several engineering domains, including applications in piezoelectric ultrasonic motors [7], doubly fed induction motors [8], 2nd-order nonlinear time-invariant plants [9], vehicle steer-by-wire systems [10], robotic manipulators [11], and wind turbine generators [12]. However, traditional PID controllers have certain limitations. For example, they are sensitive to noise, particularly in the derivative component, which can cause significant fluctuations in control signals. Additionally, they exhibit integrator windup, in which the integral term can accumulate a large value in cases of substantial errors, leading to overshooting and prolonged stabilization times. To address this, additional anti-windup schemes are required that add complexity to the control system.

Therefore, researchers and practitioners have developed variants of PID controllers to improve the performance of AVR systems. These variants comprised proportional-integral-derivative-acceleration (PIDA) [13], PID with additional second-order derivative terms ($PIDD^2$) [14-17], sigmoid PID [18], 2DOF PI controller [19], real PID with derivative filter (PIDN) [20], fractional-order PID (FOPID) controller [21], fractional order (FO) proportional-integral-derivative plus second-order derivative (FOPIDD2) [22], cascaded real proportional-integral-derivative with second order derivative and fractional-order proportional-integral (FOPI) controller [23], one plus proportional derivative with filter-fractional order proportional-integral controller [24], fractional-order proportional derivative - (one + fractional order integrator) cascade controller [25], and fuzzy tilt integral derivative with filter - one plus integral controller [26]. However, these PID variants introduce additional parameters, which increase the complexity of parameter optimization.

Therefore, researchers continue employing the PID controller for AVR systems, because it only has three parameters that need to be tuned. To achieve excellent PID controller performance, the proportional K_p, integral K_i, and derivative K_d gains must first be optimally tuned. However, tuning these parameters has posed challenges to operators and researchers, especially when using classical techniques such as Ziegler-Nichols [27], Cohen-Coon [28], and gain-phase margin [29]. These classical techniques operate by manually attempting different gains until suitable settings are obtained. However, this trial-and-error approach requires considerable effort, particularly for complicated and time-varying dynamics. Additionally, AVR systems make PID tuning even more difficult because of variable operating points and nonlinear loads. The manual tuning process struggles to find gains that work under all conditions. Overall, classical techniques are slow and often fail to find the best-fit PID gains for AVR control. Hence, better automated PID tuning is required rather than arduous manual trial-and-error techniques, particularly for systems such as the AVR, which has numerous parameter uncertainties.

Recently, researchers explored the use of modern heuristic optimization techniques to automatically tune the optimal PID gains for AVR systems. These techniques minimize the objective function to derive PID parameters. Gaing [30] pioneered the implementation of heuristic optimization algorithms to tune AVR system controllers. Gaing proposed the use of particle swarm optimization (PSO) for PID tuning of an AVR system and compared its performance with that of a genetic algorithm (GA). More recent studies have focused on the PID tuning of AVR systems using state-of-the-art metaheuristic optimization algorithms. These studies include the Lévy flight-based

reptile search algorithm [31], Runge-Kutta optimizer [32], zebra optimization algorithm [33], cuckoo search algorithm [34], sine–cosine algorithm (SCA) [35], nonlinear SCA [18], improved kidney-inspired algorithm (IKA) [36], water cycle optimization (WCO) [37], tree seed algorithm (TSA) [38], enhanced Harris hawks algorithm (EHHA) [39], equilibrium optimizer algorithm [40], hybrid simulated annealing-manta ray foraging optimization [20], artificial rabbits optimization (ARO) [41], and marine predators algorithm [21, 42].

In the aforementioned literature, metaheuristic optimization algorithms have shown excellent performance in fine-tuning PID controllers in AVR systems to maintain and stabilize the nominal voltage level of the synchronous generator. These algorithms define an objective function with criteria such as the figure of demerit (FOD), which depends on time-response specifications, including overshoot, rise time, settling time, and steady-state error [43, 44]. Additionally, a few studies utilized error-based functions, including the integral square error (ISE), integral absolute error (IAE), integral time-square error (ITSE), and integral time absolute error (ITAE) [45, 46]. However, few have incorporated robustness constraints into the objective function when tuning optimal PID controllers for AVR systems [47]. In particular, studies have incorporated robustness measures, such as the GM and PM, into the objective function by applying weights. This allows the optimization to be constrained to guarantee the desired minimum robustness. However, there is a tradeoff between robustness and performance; fixed constraints may worsen other objective function metrics. In unconstrained control optimization, robustness can be adjusted by tuning the weights of those terms. Weighting coefficients balance robustness with performance. However, selecting appropriate weights for each criterion poses challenges.

Although metaheuristic optimization algorithms can tune PID controllers for satisfactory AVR system response and robustness, parameter uncertainties are inevitable. Parameter uncertainties stemming from temperature, pressure, and other physical factors cause the actual system behavior to deviate from the theoretical results. Online manual fine-tuning of PID gains can help mitigate such issues. However, these risks compromise the robustness of the controller at its optimal value, and do not guarantee process stability. Moreover, the PID controller requires reoptimization for any new robustness constraint.

This study adopted indirect design approach-2 (IDA-2) from [48] to optimize the PID controller by adjusting a single parameter, thereby ensuring the robustness of the AVR system. IDA-2 involves the frequency-shifting of the PID controller based on a frequency-shifting constant ψ and previously optimized PID parameters. Updating ψ modifies all PID gains simultaneously, which in turn improves robustness and performance over the previously optimized PID controller. We validated the proposed approach by simulating an AVR system with a PID controller tuned via sine-cosine optimization (SCA) [35]. The relation between frequency-shifting constant ψ and robustness measures (gain margin and phase margin) was demonstrated, along with impacts on maximum sensitivity, overshoot, rise time, settling time, and FOD. The key advantage of IDA-2 is guaranteed AVR system robustness while preserving the optimized time response performance. Notably, this study presents an expanded analysis of the preliminary work in [49]. The novelty and contributions of this study are as follows:

1) The proposed method is the first to apply IDA-2 to fine-tune the optimized PID controller of an AVR system. Moreover, this study shows that the proposed PID-IDA-2 method can ensure the robustness of the AVR system during the fine-tuning process.

2) The PID-IDA-2 controller not only increases the robustness but also improves the time response of the AVR system compared to PID-SCA [35], PID-TSA [38], PID-ARO [41], PID-IKA [36], PID-EHHA [39], and PID-WCO [37].

3) This study is the first to consider the disturbance rejection and measurement noise during the parameter uncertainty of the amplifier.

The remainder of this paper is structured as follows. Section 2 explains the implementation of a PID controller in the AVR structure. Section 3 describes the procedure for applying IDA-2 to tune the PID controller. Section 4 presents the results, and Section 5 concludes the study with final remarks.

1 PID controller of AVR system

This section illustrates the overall structure of the PID controller employed in the closed-loop control of the AVR system to maintain the terminal voltage at the correct level. A comprehensive understanding of the PID controller requires a proper mathematical model of the AVR system with linearization of all components, such as the exciter, sensor, amplifier, and generator. Fig. 1 depicts the closed-loop block diagram of the AVR system with a PID controller, where K_p, K_i, and K_d represent the proportional, integral, and derivative gains, respectively. The gains of the amplifier, exciter, generator, and sensor are denoted by K_a, K_e, K_g, and K_s, respectively. Additionally, the time constants for all these

components are denoted as T_a, T_e, T_g, and T_s, respectively. The specific values of the gains and time constants were set as $K_s=1, T_s=0.01, K_g=1, T_g=1, K_e=1, T_e=0.4, K_a=10,$ and $T_a=0.1$. It is crucial to highlight that the parameter values employed in this study are aligned with those used in [35]. To mitigate issues such as saturation or other nonlinear characteristics, each component was linearized using a time constant and gain.

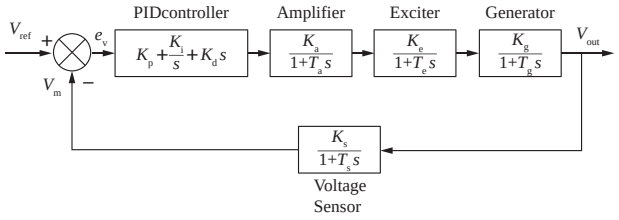

Fig. 1 Closed-loop block diagram of the automatic voltage regulator (AVR) system with the proportional–integral–derivative (PID) controller

Fundamentally, a controlled AVR system operates based on error detection. The voltage sensor transforms the output signal $V_{out}(t)$ into a measurement signal $V_m(t)$. The difference between $V_m(t)$ and $V_{ref}(t)$ is the error voltage, $e_v(t)$. The PID controller modulates the error voltage to enhance the dynamic response and eliminate steady-state errors. The amplifier then receives the output of the PID controller, which is responsible for adjusting the voltage of the exciter and operating the generator. Notably, the PID controller is distinguished by its simplicity, as it relies on only three parameters, K_p gain, K_i gain, and K_d gains, as exemplified in (1):

$$C(s)=\left(K_p+\frac{K_i}{s}+K_d s\right) \tag{1}$$

Notably, the lower and upper bounds for all gains were set to 0.2 and 2.0, respectively, based on [35]. Notably, although the performance of the PID controller may be considered satisfactory, the current PID control design for AVR systems lacks robustness to parameter uncertainty. This disadvantage warrants upgrading the design to a robust PID controller, specifically one based on the IDA-2 methodology.

2 Robust PID controller tuning based on indirect design approach-2 (IDA-2)

The proposed IDA-2 emphasizes the controller rather than process shifting, which is the focal point of the indirect design approach (IDA) theory, as described in [50]. This implies that the proposed PID tuning rules rely exclusively on the parameters of the optimized PID controller. Theorem 1 summarizes the concept of IDA-2 as described in [48]. Assuming a stable closed-loop transfer function $C(s)P(s)/(1+C(s)P(s))$ for process plant $P(s)$ and controller $C(s)$, Theorem 1 is formulated as follows:

Theorem 1 (IDA-2) [48]: The maximum sensitivity of the process decreases as the frequency-shifting constant ψ increases and vice versa. Meanwhile, the PM and GM of the open-loop transfer function $C_i(s)C_p(s-\psi)P(s)$ increase with an increase in the frequency-shifting constant ψ and vice versa, where $C_i(s)$ is the controller transfer function and $C_p(s-\psi)$ is a controller transfer function with frequency-shifted version of the process plant $P(s)$. This relationship can be mathematically expressed as follows:

$$\mathrm{GM}_{\psi_1} > \mathrm{GM}_{\psi_2} \text{ for } \psi_1 > \psi_2 \tag{2}$$

$$\mathrm{PM}_{\psi_1} > \mathrm{PM}_{\psi_2} \text{ for } \psi_1 > \psi_2 \tag{3}$$

$$M_{s,\psi_1} < M_{s,\psi_2} \text{ for } \psi_1 > \psi_2 \tag{4}$$

where $\psi \in \mathbf{R}$, $\mathrm{GM}_{\psi_1}, \mathrm{PM}_{\psi_1}$, and M_{s,ψ_1} represents the value of the GM, PM, and maximum sensitivity at ψ_i, respectively.

Proof: Here is the expression for a PID controller with proportional gain k_c, integral time constant τ_i, and derivative time constant τ_d.

$$C(s)=C_i(s)C_p(s)=\left(k_c/s\right)\left(\tau_d s^2+s+1/\tau_i\right) \tag{5}$$

This can be further simplified as

$$C(s)=\left(k_c/s\right)(s+p_1)(s+p_2) \tag{6}$$

where p_1 and p_2 are the roots of $C_p(s)$. These poles can be real or complex. Thus, a generalized expression for p_1 and p_2 can be written as

$$p_1=\alpha_r+j\alpha_i=\left(-1+\sqrt{1-4\tau_d/\tau_i}\right)/(2\tau_d),$$

$$p_2=\beta_r+j\beta_i=\left(-1+\sqrt{1-4\tau_d/\tau_i}\right)/(2\tau_d). \tag{7}$$

Substituting $C_p(s)$ with $C_p(s-\psi)$ in (5) and (6), we obtain:

$$C_{IDA2}(s)=C_i(s)C_p(s-\psi)=\left(k_c/s\right)\left(\tau_d(s-\psi)^2+(s-\psi)+1/\tau_i\right) \tag{8}$$

$$C_{IDA2}(s)=\left(k_c/s\right)\left(s+\alpha_r+j\alpha_i-\psi\right)\left(s+\beta_r+j\beta_i-\psi\right). \tag{9}$$

The GM and PM of the open-loop transfer function $G(j\omega)C_{IDA2}(j\omega)$ are defined as follows:

$$GM=1/\left|G(j\omega)C_{IDA2}(j\omega)\right|=\frac{\omega}{\left|G(j\omega)\left(\sqrt{\left((\omega+\beta_i)^2+(\beta_r-\psi)^2\right)}\times\sqrt{\left((\omega+\alpha_i)^2+(\alpha_r-\psi)^2\right)}\right)\right|} \tag{10}$$

$$PM=\pi+\angle G(j\omega)C_{IDA2}(j\omega)=\left[\pi+\angle G(j\omega)-\frac{\pi}{2}+\tan^{-1}\left(\frac{\omega+\beta_i}{\beta_r-\psi}\right)+\tan^{-1}\left(\frac{\omega+\alpha_i}{\alpha_r-\psi}\right)\right]. \tag{11}$$

By examining Eqs. (10) and (11) for

$$\psi < \min(\alpha_r, \beta_r) \tag{12}$$

the following conclusions can be drawn:

1) In (10), as the value of ψ increases, the denominator value decreases, leading to an increase in the GM, and vise versa. This relationship can be expressed mathematically as

$$\mathrm{GM}_{\psi_1} > \mathrm{GM}_{\psi_2} \text{ for } \psi_1 > \psi_2 \tag{13}$$

2) In (11), the PM of the process increases with an increase in ψ and decrease when ψ decreases. This relationship can be expressed as

$$\mathrm{PM}_{\psi_1} > \mathrm{PM}_{\psi_2} \text{ for } \psi_1 > \psi_2 \tag{14}$$

3) According to the relationship between maximum sensitivity, PM, and GM [50] is

$$M_s > GM / (GM - 1) \tag{15}$$

$$M_s > 1/\left(2\sin\left(PM / 2\right)\right) \tag{16}$$

A relationship between M_s and ψ, derived from (13) – (16) can be expressed as

$$M_{s,\psi_1} < M_{s,\psi_2} \text{ for } \psi_1 > \psi_2 \tag{17}$$

This completes the proof [48].

According to Theorem 1 [48], the PID controllers in (1) is expressed as follows:

$$C_{IDA2}(s) = \hat{K}_p + \frac{\hat{K}_i}{s} + \hat{K}_d s \tag{18}$$

where

$$\hat{K}_p = K_p - 2K_d\psi,\ \hat{K}_i = K_i + K_d\psi^2 - K_p\psi, \text{ and } \hat{K}_d = K_d. \tag{19}$$

The PID controllers derived in (18) was subsequently employed in the AVR system illustrated in Fig. 1. The objective is to assess the robustness of the proposed PID controller for the AVR system by systematically varying the frequency-shifting constant ψ along with the optimized PID parameters. In this research, the frequency-shifting constant ψ, utilized in the PID controller of the AVR system, is defined with lower and upper limits, denoted as ψ_L = –4.61 and ψ_U = 47,737.27, respectively. More importantly, these values were derived from initial investigations, ensuring stability through consistent positive values for both GM and PM.

3 Simulation results

In this section, the validity of the proposed PID tuning method is established for the PID control design of an AVR system. Its effectiveness is evaluated and compared with the optimized PID controller for the AVR system, which was tuned using the SCA [35]. Furthermore, the robustness of the proposed design method is assessed using key indicators such as the maximum sensitivity (M_s), GM, and PM of the process. In addition, a performance index based on the time-response specifications, including the maximum overshoot (M_p), rise time (T_r), settling time (T_s), and FOD, is considered. The FOD equation can be expressed as

$$\mathrm{FOD} = \left(1 - e^{-\beta}\right)\left(M_p + E_{ss}\right) + e^{-\beta}\left(T_s - T_r\right) \tag{20}$$

where M_p, E_{ss}, T_s and T_r are the maximum overshoot, steady-state error, settling time, and rise time, respectively. Notably, the FOD was chosen as the objective function because it met the designer's requirements through the weighting factor β. By setting β greater than 0.7, we can reduce the overshoot and steady-state error. Conversely, setting β less than 0.7 helps reduce the rise time and settling time. Notably, the value of β in (20) is fixed to 1.0 according to [35]. In this study, the settling time was defined as the duration required for the output response to reach 5% of the final steady-state output. The procedure for assessing the robustness of a PID controller for an AVR system is outlined as follows:

(1) The PID controller was initially designed using established optimal tuning techniques, that is, SCA, as outlined in [35]. The optimized PID controller gains obtained using the SCA were K_p = 0.9826, K_i = 0.8337, and K_d = 0.4982.

(2) Subsequently, the PID controller optimized in [35] was fine-tuned using the proposed IDA-2 method to enhance robustness.

(3) The effectiveness of IDA-2 was demonstrated in the context of diverse parameter uncertainties.

(4) The effectiveness of the proposed PID-IDA-2 method was further tested by introducing disturbances and measurement noise amid parameter uncertainty (K_a = 15) and comparing the results with those of PID-SCA [35], PID-TSA [38], PID-ARO [41], PID-IKA [36], PID-EHHA [39], and PID-WCO [37].

(5) A frequency response analysis was conducted to evaluate the robustness of the PID-IDA-2 method against existing methods.

Table 1 presents the results of PID tuning based on IDA-2 for uncertainties in the amplifier parameters, considering various values of T_a (0.097, 0.12, 0.13, and 0.15) and K_a (9.7, 12, 13, and 15). The performance indices in (19) are examined by varying ψ, where the results for $\psi = 0$ refer to the existing optimized PID parameters in [35]. Table 1 also lists the values of PID parameters (K_p, K_i, and K_d) for each variation of ψ, which are recalculated based on (19). The table demonstrates that the online tuning of the PID controller enables users to adjust the controller's robustness in real time, resulting in a superior transient response of the AVR system compared to the optimized PID controller, especially under parameter uncertainties.

As evident in Table 1, changing the value of ψ influences the robustness of the controller, as proposed in Theorem 1. When ψ increases from –0.05 to 0.05 for both T_a and K_a uncertainties, the values of GM and PM increase. In the case of T_a = 0.097, GM and PM increase by approximately 0.4% and 1.3%, respectively, as ψ increases from 0 to 0.05. Similar trends are observed for other parameter uncertainties, such as for T_a = 0.12, where GM and PM increase by approximately 0.48% and 1.45%, respectively. Furthermore, the positive change in T_a contributes to a more stable AVR system, resulting in a smaller maximum sensitivity M_s and a higher GM for the nominal case ($\psi = 0$). As observed in Table 1, the GM increases by approximately 0.5%, 0.8%, and 1.5% for T_a = 0.12, T_a = 0.13, and T_a = 0.15, respectively. Meanwhile, M_s decreases by approximately 2.4%, 3.4%, and 5.1% for T_a = 0.12, T_a = 0.13, and T_a = 0.15, respectively. Additionally, marginal improvements in the values of FOD and M_p can be observed at larger ψ for every positive change of T_a. In the case of T_a = 0.13, the FOD and M_p decrease by approximately 1% as ψ increases from 0 to 0.05. However, T_s and T_s gradually increase with the increase of ψ. In the case of T_a = 0.15, T_s and T_s increase by approximately 1.3% and 1.1%, respectively, as ψ increases from 0 to 0.05.

Conversely, an increase in K_a makes the AVR system less stable, leading to a higher M_s and smaller GM and PM for the nominal case ($\psi = 0$). As observed in Table 1, GM decreases by approximately 9%, 0.8%, and 1.5% for K_a = 12, K_a = 13, and K_a = 15, respectively. Meanwhile, M_s increases by approximately 3.9%, 5.7%, and 8.9% for K_a = 12, K_a = 13, and K_a = 15, respectively. Despite this, an increase in ψ leads to slight improvements in FOD and M_p for every positive change in K_a. In the case of K_a = 13, FOD and M_p decrease by about 1.3% and 0.8%, respectively, as ψ increases from 0 to 0.05. Nonetheless, T_s and T_r also gradually increase with the increment of ψ. In the case of K_a = 15, T_s and T_r increase by approximately 0.8% and 0.5%, respectively, as ψ increases from 0 to 0.05.

Table 2 presents the results of PID tuning based on IDA-2 for uncertainties in the generator parameters, considering a varying T_g (0.8. 0.97, 1.1, and 1.5) and K_g (0.97, 1.2, 1.3, and 1.5). Notably, the values of GM and PM increase as ψ increases from –0.05 to 0.05 amid parameter uncertainties of both T_g and K_g. In the case of T_g= 0.8, GM and PM increase by approximately 0.4% and 1.2%, respectively, as ψ increases from 0 to 0.05. Similar patterns are observed for other parameter uncertainties, such as for T_g= 0.97, where GM and PM increase by approximately 0.41% and 1.3%, respectively. Additionally, a positive change in T_g contributes to a more stable AVR system, resulting in a smaller maximum sensitivity M_s and a higher GM and PM for the nominal case ($\psi = 0$). Specifically, as evident in Table 2, the GM increased by approximately 8%, 13.4%, and 26.8% for T_g= 0.97, T_g = 1.1, and T_g = 1.5, respectively. Meanwhile, M_s decreased by approximately 3.4%, 5.2%, and 9.5% at T_g = 0.97, T_g = 1.1, and T_g = 1.5, respectively. Additionally, there are slight improvements in the values of FOD and M_p when a larger ψ is applied for every positive change of T_g. In the case of T_g = 1.5, FOD and M_p decrease by approximately 13.9% and 0.1%, respectively, as ψ increases from 0 to 0.05. However, T_s and T_r gradually increase with ψ. In the case of T_g = 1.1, the T_s and T_r increase by approximately 2.9% and 1.1%, respectively, as ψ increases from 0 to 0.05.

Conversely, an increase in K_g reduces the stability of the AVR system, leading to a higher M_s and smaller GM and PM for the nominal case ($\psi = 0$). As shown in Table 2, GM decreases by approximately 9%, 12.4%, and 18.4% for K_g = 1.2, K_g = 1.3, and K_g = 1.5, respectively. Meanwhile, M_s increases by approximately 3.9%, 5.7%, and 8.9% for K_g = 1.2, K_g = 1.3, and K_g = 1.5, respectively. Nonetheless, with an increment in ψ, the FOD and M_p slightly improve for every positive change in K_g. In the case of K_g= 1.3, FOD and M_p decrease by approximately 1.3% and 0.8%, respectively, as ψ increases from 0 to 0.05. Nevertheless, T_s and T_r gradually increase with an increase in ψ. In the case of K_g = 1.5, T_s and T_r increase by approximately 0.7% and 0.5%, respectively, as ψ increases from 0 to 0.05.

The results in Table 1 and Table 2 collectively demonstrate that a larger positive value of ψ significantly improves the robustness of the PID controller for the AVR system, as proven by the GM and PM results. This observation aligns with Theorem 1 of [48].

Figure 2 presents a three-dimensional (3D) plot of the relationship between T_a, ψ, and GM. As evident in the plot, increments in T_a and ψ results in an increase in the GM. Simultaneously, Fig. 3 displays a 3D plot of the relationship between T_a, ψ, and PM. The plot clearly illustrates that PM is directly proportional to ψ and inversely proportional to T_a. In simpler terms, as ψ increases, PM increases, while an increase in T_a leads to a decrease in PM.

Figure 4 depicts a 3D plot of the relationship between K_a, ψ, and GM. As evident in the figure, the GM is directly proportional to ψ and inversely proportional to K_a. To elaborate, GM increases as ψ increases, while GM decreases with an increase in K_a. Simultaneously, Fig. 5 exhibits a 3D plot of the relationship between K_a, ψ, and PM. This plot demonstrates that PM is directly proportional to ψ and inversely proportional to K_a. In simpler terms, as ψ increases, the PM increases, while an increase in K_a

Table 1 Outcomes of proportional–integral–derivative (PID) tuning, utilizing the proposed IDA-2 method, considering uncertainties in the amplifier's parameters (T_a and K_a) for the automatic voltage regulator (AVR) system

Parameter uncertainty	ψ	K_p	K_i	K_d	T_s/s	T_r/s	M_p/V	FOD	M_s/dB	GM/dB	PM/°
	−0.05	1.0324	0.8841	0.4982	0.7010	0.1455	1.1204	0.2805	1.2634	20.2084	52.3812
	−0.01	0.9926	0.8436	0.4982	0.7134	0.1465	1.1117	0.2792	1.2624	20.2741	52.9198
T_a = 0.097	0.00	0.9826	0.8337	0.4982	0.7168	0.1467	1.1095	0.2789	1.2621	20.2905	53.0545
	0.01	0.9726	0.8239	0.4982	0.7202	0.1470	1.1073	0.2787	1.2618	20.3068	53.1891
	0.05	0.9328	0.7858	0.4982	0.7351	0.1481	1.0985	0.2782	1.2608	20.3717	53.7279
	−0.05	1.0324	0.8841	0.4982	0.7656	0.1550	1.1523	0.3209	1.2323	20.2994	49.2511
	−0.01	0.9926	0.8436	0.4982	0.7752	0.1561	1.1431	0.3182	1.2315	20.3769	49.8301
T_a = 0.12	0.00	0.9826	0.8337	0.4982	0.7777	0.1563	1.1408	0.3176	1.2313	20.3962	49.9750
	0.01	0.9726	0.8239	0.4982	0.7803	0.1566	1.1385	0.3170	1.2311	20.4154	50.1198
	0.05	0.9328	0.7858	0.4982	0.7918	0.1577	1.1291	0.3149	1.2302	20.4940	50.6993
	−0.05	1.0324	0.8841	0.4982	0.7925	0.1589	1.1640	0.3367	1.2199	20.3538	48.1510
	−0.01	0.9926	0.8436	0.4982	0.8010	0.1602	1.1538	0.3329	1.2191	20.4362	48.7472
T_a = 0.13	0.00	0.9826	0.8337	0.4982	0.8034	0.1606	1.1512	0.3320	1.2189	20.4567	48.8964
	0.01	0.9726	0.8239	0.4982	0.8057	0.1609	1.1486	0.3312	1.2188	20.4772	49.0455
	0.05	0.9328	0.7858	0.4982	0.8161	0.1621	1.1392	0.3286	1.2180	20.5586	49.6424
	−0.05	1.0324	0.8841	0.4982	0.8440	0.1665	1.1842	0.3657	1.1986	20.4785	46.2985
	−0.01	0.9926	0.8436	0.4982	0.8510	0.1677	1.1744	0.3616	1.1977	20.5705	46.9284
T_a = 0.15	0.00	0.9826	0.8337	0.4982	0.8529	0.1680	1.1719	0.3606	1.1975	20.5934	47.0859
	0.01	0.9726	0.8239	0.4982	0.8548	0.1683	1.1694	0.3597	1.1973	20.6162	47.2437
	0.05	0.9328	0.7858	0.4982	0.8636	0.1698	1.1593	0.3559	1.1964	20.7068	47.8742
	−0.05	1.0324	0.8841	0.4982	0.7191	0.1506	1.1156	0.2822	1.2536	20.4816	52.8348
	−0.01	0.9926	0.8436	0.4982	0.7324	0.1517	1.1066	0.2810	1.2526	20.5489	53.3919
K_a = 9.7	0.00	0.9826	0.8337	0.4982	0.7360	0.1520	1.1043	0.2808	1.2524	20.5656	53.5313
	0.01	0.9726	0.8239	0.4982	0.7396	0.1523	1.1020	0.2805	1.2522	20.5823	53.6706
	0.05	0.9328	0.7858	0.4982	0.7553	0.1538	1.0934	0.2803	1.2512	20.6488	54.2280
	−0.05	1.0324	0.8841	0.4982	0.6540	0.1252	1.1804	0.3086	1.3021	18.6334	46.5838
	−0.01	0.9926	0.8436	0.4982	0.6603	0.1259	1.1725	0.3056	1.3013	18.7007	47.0577
K_a = 12	0.00	0.9826	0.8337	0.4982	0.6620	0.1260	1.1705	0.3049	1.3011	18.7174	47.1762
	0.01	0.9726	0.8239	0.4982	0.6638	0.1263	1.1685	0.3042	1.3009	18.7341	47.2947
	0.05	0.9328	0.7858	0.4982	0.6715	0.1272	1.1603	0.3016	1.3000	18.8007	47.7686
	−0.05	1.0324	0.8841	0.4982	0.6300	0.1170	1.2059	0.3189	1.3248	17.9382	44.3322
	−0.01	0.9926	0.8436	0.4982	0.6348	0.1176	1.1980	0.3154	1.3239	18.0054	44.7796
K_a = 13	0.00	0.9826	0.8337	0.4982	0.6361	0.1178	1.1960	0.3146	1.3237	18.0222	44.8914
	0.01	0.9726	0.8239	0.4982	0.6374	0.1180	1.1940	0.3137	1.3234	18.0389	45.0033
	0.05	0.9328	0.7858	0.4982	0.6433	0.1190	1.1859	0.3104	1.3225	18.1054	45.5406
	−0.05	1.0324	0.8841	0.4982	0.5885	0.1048	1.2518	0.3371	1.3646	16.6952	40.4387
	−0.01	0.9926	0.8436	0.4982	0.5913	0.1052	1.2442	0.3332	1.3636	16.7625	40.8437
K_a = 15	0.00	0.9826	0.8337	0.4982	0.5921	0.1054	1.2423	0.3322	1.3633	16.7792	40.9450
	0.01	0.9726	0.8239	0.4982	0.5928	0.1055	1.2403	0.3312	1.3631	16.7959	41.0462
	0.05	0.9328	0.7858	0.4982	0.5963	0.1059	1.2325	0.3274	1.3621	16.8625	41.4511

Table 2 Outcomes of PID tuning, utilizing the IDA-2 method, considering uncertainties in the generator's parameters (T_g and K_g) for the AVR system

Parameter uncertainty	ψ	K_p	K_i	K_d	T_s(s)	T_s/s	T_r/s	M_p/V	FOD	M_s/dB	GM/dB
	−0.05	1.0324	0.8841	0.4982	0.6623	0.1233	1.1674	0.3041	1.3084	18.4876	46.8626
	−0.01	0.9926	0.8436	0.4982	0.6699	0.1240	1.1598	0.3019	1.3089	18.5535	47.3243
T_g = 0.8	0.00	0.9826	0.8337	0.4982	0.6723	0.1241	1.1579	0.3015	1.3089	18.5698	47.4397
	0.01	0.9726	0.8239	0.4982	0.6746	0.1244	1.1560	0.3010	1.3090	18.5862	47.5551
	0.05	0.9328	0.7858	0.4982	0.6845	0.1253	1.1483	0.2994	1.3091	18.6513	48.0168
	−0.05	1.0324	0.8841	0.4982	0.7048	0.1432	1.1301	0.2889	1.2661	19.9785	51.2088
	−0.01	0.9926	0.8436	0.4982	0.7160	0.1444	1.1219	0.2873	1.2651	20.0456	51.7403
T_g = 0.97	0.00	0.9826	0.8337	0.4982	0.7191	0.1447	1.1198	0.2870	1.2649	20.0623	51.8732
	0.01	0.9726	0.8239	0.4982	0.7222	0.1449	1.1177	0.2868	1.2646	20.0790	52.0061
	0.05	0.9328	0.7858	0.4982	0.7358	0.1460	1.1093	0.2860	1.2636	20.1453	52.5378
	−0.05	1.0324	0.8841	0.4982	0.7185	0.1583	1.1072	0.2739	1.2416	20.9679	54.1603
	−0.01	0.9926	0.8436	0.4982	0.7341	0.1597	1.0981	0.2733	1.2408	21.0357	54.7460
T_g = 1.1	0.00	0.9826	0.8337	0.4982	0.7382	0.1601	1.0958	0.2732	1.2406	21.0526	54.8924
	0.01	0.9726	0.8239	0.4982	0.7423	0.1604	1.0935	0.2732	1.2404	21.0694	55.0389
	0.05	0.9328	0.7858	0.4982	0.7595	0.1618	1.0844	0.2732	1.2396	21.1365	55.6251
	−0.05	1.0324	0.8841	0.4982	0.4386	0.2057	1.0541	0.1199	1.1853	23.4540	61.6865
	−0.01	0.9926	0.8436	0.4982	0.2869	0.2082	1.0439	0.0567	1.1847	23.5232	62.4458
T_g = 1.5	0.00	0.9826	0.8337	0.4982	0.2880	0.2090	1.0413	0.0552	1.1846	23.5405	62.6359
	0.01	0.9726	0.8239	0.4982	0.2890	0.2098	1.0387	0.0536	1.1844	23.5577	62.8261
	0.05	0.9328	0.7858	0.4982	0.2933	0.2130	1.0284	0.0475	1.1838	23.6261	63.5880
	−0.05	1.0324	0.8841	0.4982	0.7191	0.1506	1.1156	0.2822	1.2536	20.4816	52.8348
	−0.01	0.9926	0.8436	0.4982	0.7324	0.1517	1.1066	0.2810	1.2526	20.5489	53.3919
K_g = 0.97	0.00	0.9826	0.8337	0.4982	0.7360	0.1520	1.1043	0.2808	1.2524	20.5656	53.5313
	0.01	0.9726	0.8239	0.4982	0.7396	0.1523	1.1020	0.2805	1.2522	20.5823	53.6706
	0.05	0.9328	0.7858	0.4982	0.7553	0.1538	1.0934	0.2803	1.2512	20.6488	54.2280
	−0.05	1.0324	0.8841	0.4982	0.6540	0.1252	1.1804	0.3086	1.3021	18.6334	46.5838
	−0.01	0.9926	0.8436	0.4982	0.6603	0.1259	1.1725	0.3056	1.3013	18.7007	47.0577
K_g = 1.2	0.00	0.9826	0.8337	0.4982	0.6620	0.1260	1.3011	0.3049	1.3011	18.7174	47.1762
	0.01	0.9726	0.8239	0.4982	0.6638	0.1263	1.1685	0.3042	1.3009	18.7341	47.2947
	0.05	0.9328	0.7858	0.4982	0.6715	0.1272	1.1603	0.3016	1.3000	18.8007	47.7686
	−0.05	1.0324	0.8841	0.4982	0.6300	0.1170	1.2059	0.3189	1.3248	17.9382	44.3322
	−0.01	0.9926	0.8436	0.4982	0.6348	0.1176	1.1980	0.3154	1.3239	18.0054	44.7796
K_g = 1.3	0.00	0.9826	0.8337	0.4982	0.6361	0.1178	1.1960	0.3146	1.3237	18.0222	44.8914
	0.01	0.9726	0.8239	0.4982	0.6374	0.1180	1.1940	0.3137	1.3234	18.0389	45.0033
	0.05	0.9328	0.7858	0.4982	0.6433	0.1190	1.1859	0.3104	1.3225	18.1054	45.4506
	−0.05	1.0324	0.8841	0.4982	0.5885	0.1048	1.2518	0.3371	1.3646	16.6952	40.4387
	−0.01	0.9926	0.8436	0.4982	0.5913	0.1052	1.2442	0.3332	1.3636	16.7625	40.8437
K_g = 1.5	0.00	0.9826	0.8337	0.4982	0.5921	0.1054	1.2423	0.3322	1.3633	16.7792	40.9450
	0.01	0.9726	0.8239	0.4982	0.5928	0.1055	1.2403	0.3312	1.3631	16.7959	41.0462
	0.05	0.9328	0.7858	0.4982	0.5963	0.1059	1.2325	0.3274	1.3621	16.8625	41.4511

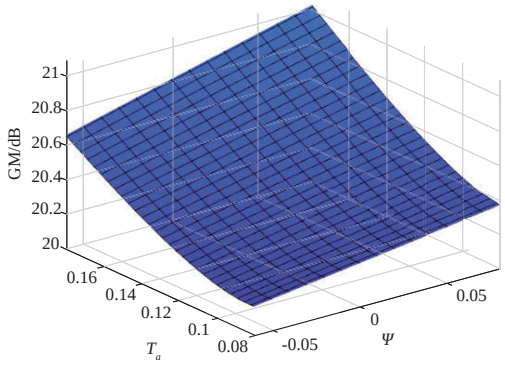

Fig. 2 Three-dimensional (3D) plot of T_a vs. ψ vs. GM

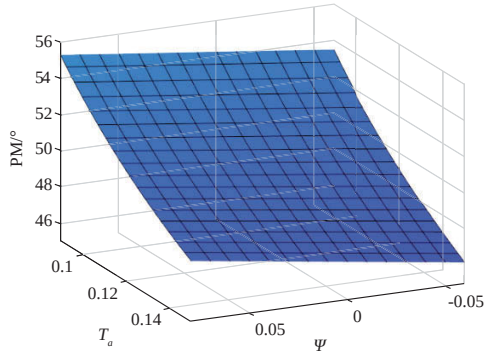

Fig. 3 3D plot of T_a vs. ψ vs. PM

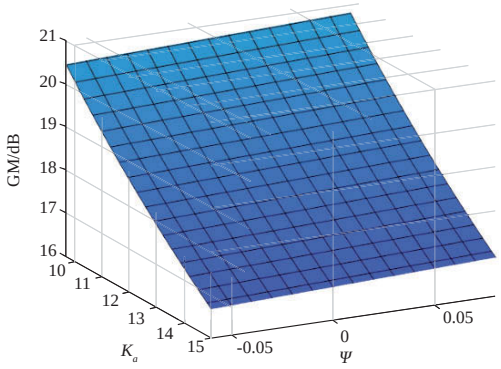

Fig. 4 3D plot of K_a vs. ψ vs. GM

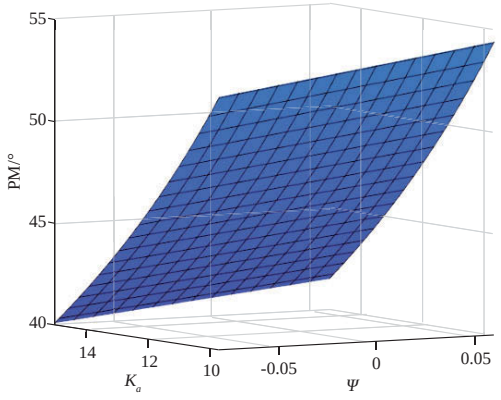

Fig. 5 3D plot of K_a vs. ψ vs. PM

results in a decrease in the PM.

Additionally, Fig. 6 presents a 3D plot of the relationship between T_g, ψ, and GM. In this figure, the GM is directly proportional to both ψ and T_g. Meanwhile, Fig. 7 displays a 3D plot of the relationship between T_g, ψ, and PM. Here, PM is directly proportional to both ψ and T_g.

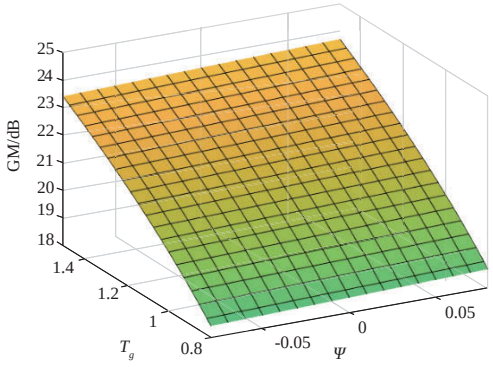

Fig. 6 3-D plot of T_g vs. ψ vs. GM

Figure 8 displays the AVR system responses generated by the PID-SCA [35] and PID-IDA-2 controller at a

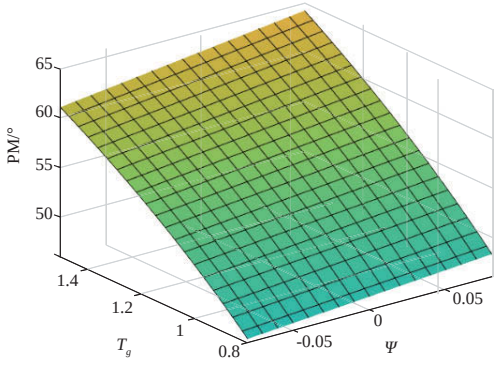

Fig. 7 3D plot of T_g vs. ψ vs. PM

reference of 1 per unit (p.u.) and a simulation time of 5 s. The AVR responses from both controllers were recorded under parameter uncertainties of T_a = 0.15, K_a = 15, T_g = 1.5, and K_g = 1.5. Specifically, for PID-IDA-2, the ψ values are configured as [–0.05, –0.01, 0.01, 0.05]. Notably, the PID-SCA response is replicated by directly using the PID parameters from the respective studies. Examining the time response in Fig. 8 reveals that, with each parameter uncertainty, increasing ψ leads to a reduction in M_p. This result shows that the ψ = 0.05 yields the best results for all parameter uncertainty cases by scoring the lowest value of M_p. Although slight increments in T_s and T_r occur in all parameter uncertainty cases, an overall improvement in the objective function FOD was evident, as indicated in Table 1 and Table 2.

As evidenced by improvements in terms of M_s, GM, and PM, augmenting the frequency-shifting constant ψ appears to enhance the robustness of the AVR system. The inclusion of ψ also proves effective in preserving a robust AVR response even amid system parameter uncertainties. Overall, the proposed IDA-2 method emerges as a suitable tool for PID controller tuning, demonstrating commendable attributes in terms of both robustness and simplicity.

Moreover, to compare the effectiveness of the proposed method with a state-of-the-art controller, we considered [3] and [51], who proposed a sliding mode controller (SMC) and FLC, respectively. Notably, the comparison was performed without subjecting the AVR to any parameter uncertainty. Table 3 lists the time-response specifications in terms of percentage overshoot (%*OS*), rise time (T_r), and settling time (T_s) for PID-IDA-2 (ψ = 0.05), SMC [3], and FLC [51]. The results show that the proposed PID-IDA-2 method achieves faster T_r and T_s than SMC and FLC. However, in terms of %*OS*, PID-IDA-2 ranked third behind FLC and SMC. Overall, PID-IDA-2 demonstrates competitive performance compared with state-of-the-art controllers.

Table 3 Time-response specification results for PID-IDA-2 (ψ = 0.05), SMC [3], and FLC [51]

Controller	%/OS	T_r/s	T_s/s
PID-IDA-2	10.33	0.1495	0.7423
SMC [3]	0.09	0.3441	0.8635
FLC [51]	0	1.032	1.028

Furthermore, the effectiveness of the PID-IDA-2 method was tested by introducing disturbances during the parameter uncertainty (K_a = 15). To test the rapid reactions to disturbances, a step input was applied to the AVR system.

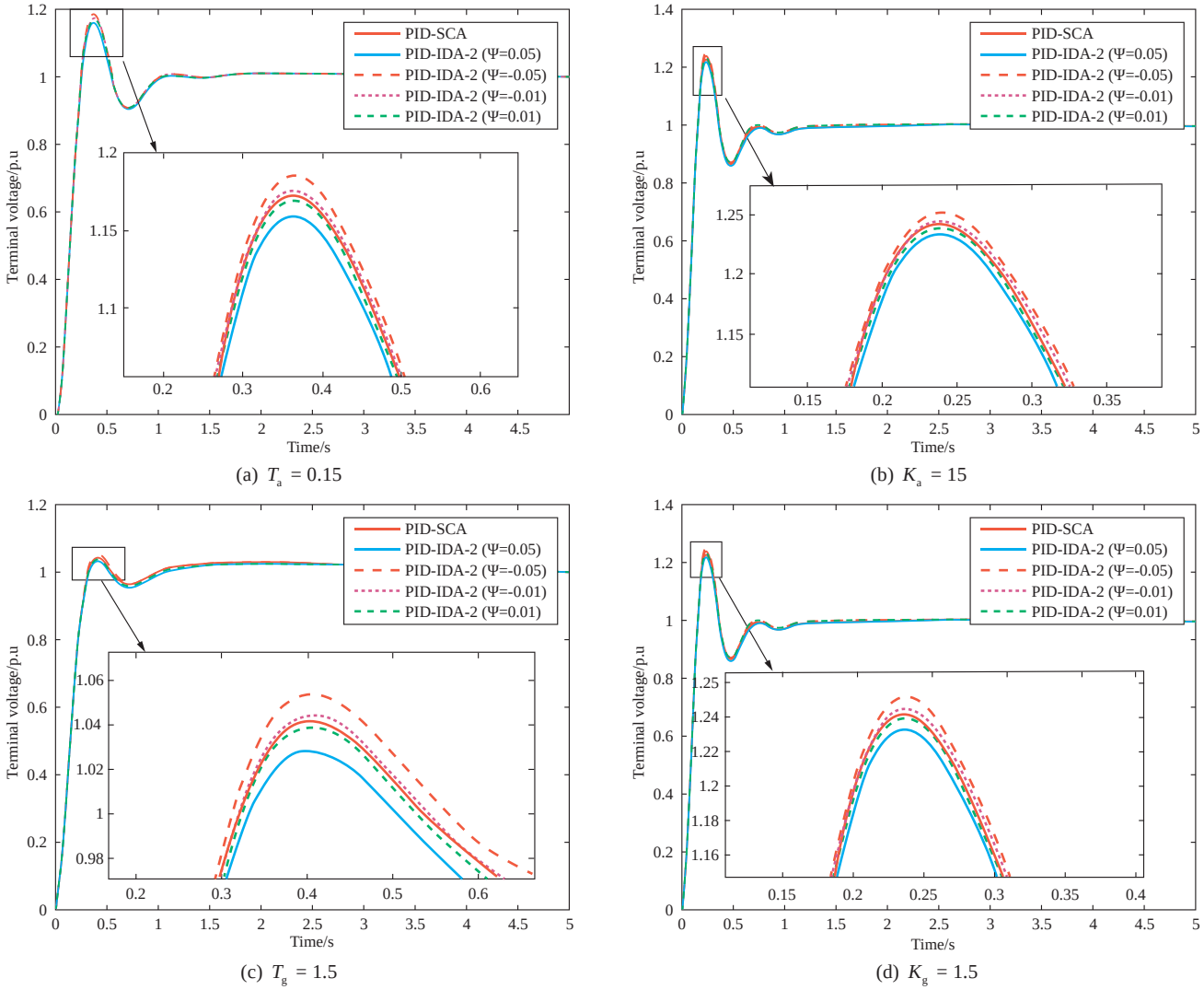

(a) T_a = 0.15 (b) K_a = 15

(c) T_g = 1.5 (d) K_g = 1.5

Fig. 8 AVR system responses produced by PID-SCA [35] and PID-IDA-2 (ψ = [-0.05, -0.01, 0.01, 0.05]) for various parameter uncertainties (a) T_a = 0.15, (b) K_a = 15, (c) T_g = 1.5, and (d) K_g = 1.5

Then, at t = 1 and 3 s, the disturbances with amplitudes 0.5 and –0.5, respectively, are applied to the output voltage. Fig. 9 shows the AVR system responses with disturbance rejection amid parameter uncertainties (K_a = 15) produced by PID-IDA-2 (ψ = 0.05), PID-SCA [35], PID-TSA [38], PID-ARO [41], PID-IKA [36], PID-EHHA [39], and PID-WCO [37]. Notably, the PID controller parameters for PID-SCA, PID-TSA, PID-ARO, PID-IKA, PID-EHHA, and PID-WCO were directly adopted from their respective studies, as listed in Table 4. As shown in Fig. 9, PID-IDA-2 can react to disturbances better than the other methods. This can be proven by the performance indices in terms of the ISE, IAE, ITSE, and ITAE, as listed in Table 5. As shown in the table, PID-IDA-2 produces competitive results by obtaining the lowest ISE value alongside PID-EHHA, followed by PID-IKA, PID-SCA, PID-TSA, PID-ARO, and PID-WCO. It also obtained the lowest IAE value compared to the other methods. Meanwhile, for ITSE and ITAE, PID-IDA-2 achieved the second lowest value, following PID-ARO. This was followed by PID-SCA, PID-TSA, PID-IKA, PID-EHHA, and PID-WCO.

Table 4 Comparison of PID controller parameters for AVR system

Algorithm	K_p	K_i	K_d
IDA-2	0.9328	0.7858	0.4982
SCA [35]	0.9826	0.8337	0.4982
TSA [38]	1.1281	0.9567	0.5671
ARO [41]	1.0386	0.6748	0.3808
IKA [36]	1.0426	1.0093	0.5999
EHHA [39]	0.8764	0.5678	0.6536
WCO [37]	1.4802	1.0153	0.4809

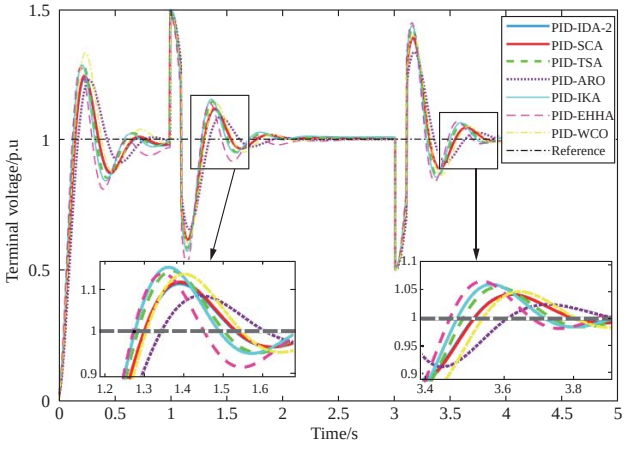

Fig. 9 AVR system responses with disturbance rejection amid parameter uncertainties (K_a = 15)

Table 5 ISE, IAE, ITSE, and ITAE produced by all methods for disturbance rejection amid parameter uncertainties (K_a= 15)

Controller	Param. Uncertain.	ISE	IAE	ITSE	ITAE
PID-IDA-2		0.1472	0.3884	0.1425	0.5513
PID-SCA [35]		0.148	0.3894	0.1437	0.5523
PID-TSA [38]		0.1494	0.3995	0.1522	0.5746
PID-ARO [41]	K_a = 15	0.1567	0.3939	0.1412	0.5339
PID-IKA [36]		0.1479	0.4002	0.1526	0.5810
PID-EHHA [39]		0.1472	0.4103	0.1545	0.5995
PID-WCO [37]		0.1598	0.4224	0.1583	0.5969

In addition, measurement noise was added to the AVR system to further evaluate the effectiveness of each controller during parameter uncertainty (K_a = 15). White noise with a noise power of 0.001 was used as the measurement noise. Fig. 10 illustrates the AVR response amid measurement noise obtained by PID-IDA-2 (ψ = 0.05), PID-SCA [35], PID-TSA [38], PID-ARO [41], PID-IKA [36], PID-EHHA [39], and PID-WCO [37]. As evident from this response, PID-IDA-2's response can follow the reference signal satisfactorily. Table 6 lists the numerical results of all performance indices obtained by all algorithms. The table shows that the PID-IDA-2 controller produces highly competitive results by obtaining the second-lowest values for ITSE, second to PID-EHHA. For the IAE and ITAE results, PID-IDA-2 produces the third-lowest values for PID-IKA and PID-EHHA. For ISE, PID-IDA-2 scored the fourth lowest value, followed by PID-EHHA in first place, PID-IKA in the second place, and PID-TSA in the third place. In essence, although the AVR system is subjected to measurement noise during the trajectory tracking simulation, the PID-IDA-2 controller can still cater to it, proving that this method is the most efficient and robust.

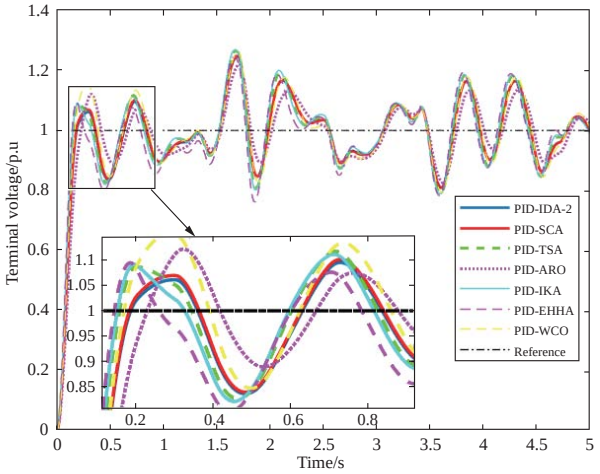

Fig. 10 AVR system responses amid measurement noise and parameter uncertainties (K_a = 15)

Table 6 ISE, IAE, ITSE, and ITAE produced by all controllers amid measurement noise and parameter uncertainties (K_a= 15)

Controller	Param. Uncertain.	ISE	IAE	ITSE	ITAE
PID-IDA-2		0.1333	0.5292	0.1636	1.1150
PID-SCA [35]		0.1340	0.5308	0.1655	1.1220
PID-TSA [38]		0.1332	0.5334	0.1687	1.1360
PID-ARO [41]	K_a = 15	0.1409	0.5328	0.1674	1.1130
PID-IKA [36]		0.1306	0.5277	0.1643	1.1210
PID-EHHA [39]		0.1283	0.5238	0.1582	1.0990
PID-WCO [37]		0.1460	0.5697	0.1901	1.2140

Finally, the frequency response analysis of PID-IDA-2 and other methods was conducted using a Bode plot with parameter uncertainties (K_a = 15). The stability characteristics were analyzed from the Bode plot by analyzing the GM and PM. Generally, an AVR system is said to be stable if GM and PM are positive, whereas a system with larger GM and PM is considered more stable. In particular, the stability performance of the system using PID-IDA-2 was compared with PID-SCA [35], PID-TSA [38], PID-ARO [41], PID-IKA [36], PID-EHHA [39], and PID-WCO [37]. Fig. 11 shows the Bode plots of magnitude and phase for PID-IDA-2 and other methods, while Table 7 lists the GM and PM results obtained by all methods. According to the results, PID-IDA-2 obtained highly competitive results by scoring the second-highest GM and PM values of 16.8625 and 41.4511, respectively. These values were less than 10% of the highest value produced by the PID-ARO. The third highest GM value was produced by PID-SCA, followed by PID-WCO, PID-TSA, PID-IKA, and PID-EHHA. Overall, PID-IDA-2 has produced a good frequency response by considering the second highest GM and PM values.

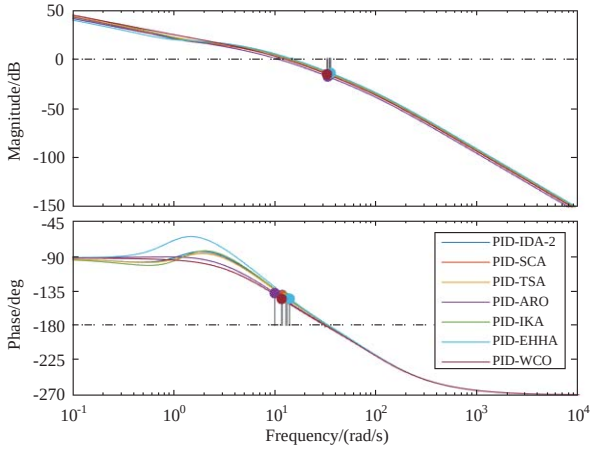

Fig. 11 Bode plots for AVR systems during the parameter uncertainty (K_a = 15)

Table 7 The GM and PM produced by all controllers during the parameter uncertainty (K_a= 15)

Controller	Param. Uncertain.	GM	PM
PID-IDA-2		16.8625	41.4511
PID-SCA [35]		16.7792	40.9450
PID-TSA [38]		15.6399	37.4406
PID-ARO [41]	K_a = 15	18.4551	43.8105
PID-IKA [36]		15.3609	37.1464
PID-EHHA [39]		14.9324	36.5586
PID-WCO [37]		16.1074	36.1228

4 Conclusion

This study introduces a novel PID tuning approach for an AVR system that exploits IDA-2 to enhance its robustness and performance. The key concept involves single-parameter adjustment of the frequency-shifting constant in an optimized PID control method. This modification provides an additional capability for online robustness and control performance adjustments. The proposed fine-tuning rules are independent of the process model and are derived from a previously optimized PID controller for AVR systems. The effect of tuning the frequency-shifting constant on the PID controller of the AVR system is demonstrated through simulation results. These findings indicate that a large positive value of the frequency-shifting constant significantly improves the controller's robustness. Moreover, the simulation results revealed that PID-IDA-2 can produce a good time response even when the AVR system is subject to disturbances and measurement noise amid parameter uncertainties. Additionally, the frequency response analysis showed that PID-IDA-2 obtained competitive results compared to the other methods. However, it is currently only applicable to specific frequency-shifting constants. Future studies should explore the implementation of an adaptive frequency-shifting constant within the proposed stability range to address various PID controller challenges. Furthermore, the proposed method can be applied to other energy conversion systems if the PID controller parameters for those systems are available.

Acknowledgments

The authors express their gratitude to the Malaysian Ministry of Higher Education (MOHE) for their support through the Fundamental Research Grant Scheme (FRGS/1/2021/ICT02/UMP/03/3) (UMPSA Reference:

RDU 210117). Additionally, appreciation is extended to Universiti Malaysia Pahang Al-Sultan Abdullah for providing the necessary laboratory facilities. Additionally, heartfelt thanks are extended to Universiti Teknikal Malaysia Melaka for their invaluable assistance in completing this paper.

Declaration of competing interest

We declare that we have no conflict of interest.

References

[1] Ayas M S, Sahin A K (2023) A reinforcement learning approach to Automatic Voltage Regulator system. Engineering Applications for Artificial Intelligence, 121: 106050

[2] Gupta T, Sambariya D.K (2017) Optimal design of fuzzy logic controller for automatic voltage regulator. International Conference on Information, Communication, Instrumentation and Control (ICICIC), pp: 1-6

[3] Furat M, Cucu G G (2022) Design, implementation, and optimization of sliding mode controller for automatic voltage regulator system. IEEE Access, 10: 55650-55674

[4] Lawal M J, Hussein S U, Saka B, et al. (2023) Attah, Intelligent fuzzy-based automatic voltage regulator with hybrid optimization learning method. Science African, 19

[5] Saat S, Ghazali M R, Ahmad M A, et al. (2023) An implementation of brain emotional learning based intelligent controller for AVR system. 2023 IEEE International Conference on Automatic Control and Intelligent Systems (I2CACIS), Shah Alam, Malaysia, pp: 60-64

[6] Borase, R P, Maghade D K, Sondkar S Y, et al. A review of PID control, tuning methods and applications. International Journal of Dynamic and Control, 9(5): 818–827

[7] Makarem S, Delibas B, Koc B (2021) Data-driven tuning of PID controlled piezoelectric ultrasonic motor. Actuators, 10(7): 148

[8] Mahfoud S, Derouich A, El Ouanjli N, et al. (2021) Improved DTC of the PID controller by using genetic algorithm of a doubly fed induction motor. Lecture Notes in Networks and Systems. Springer International Publishing, pp: 1687-1698

[9] Yu H, Guan Z, Chen T, et al. Design of data-driven PID controllers with adaptive updating rules. Automatica, 121:109185

[10] Tumari M Z, Saealal M S, Rashid W N, et al. (2017). The Vehicle steer by wire control system by implementing PID controller. Journal of Telecommunication, Electronic and Computer Engineering, 9: 43-47.

[11] Su Y, Zheng C (2017) PID control for global finite-time regulation of robotic manipulators. International Journal of Systems Science, 48(3):1-12

[12] Ramesh M, Yadav A K, Pathak P K (2022) Artificial gorilla troops optimizer for frequency regulation of wind contributed microgrid system. Journal of Computational and Nonlinear Dynamics, 18(1): 011005

[13] Mosaad A M., Mahmoud A A, Almoataz Y A (2019) Whale optimization algorithm to tune PID and PIDA controllers on AVR system. Ain Shams Engineering Journal, 10(4): 755-767

[14] Sahib, Mouayad A A (2015) novel optimal PID plus second order derivative controller for AVR system. Engineering Science and Technology an International Journal, 13(2): 194-206

[15] Izci D, Ekinci S, Mirjalili S (2023) Optimal PID plus second-order derivative controller design for AVR system using a modified Runge Kutta optimizer and Bode's ideal reference model. International Journal of Dynamics and Control, 11: 1247-1264

[16] Ekinci S, Izci D, Eker E, et al. (2023) An effective control design approach based on novel enhanced aquila optimizer for automatic voltage regulator. Artificial Intelligence Review, 56: 1731–1762

[17]Izci D, Ekinci S, Mirjalili S, et al. (2023) An intelligent tuning scheme with a master/slave approach for efficient control of the automatic voltage regulator. Neural Computing and Applications, 35(26): 19099-19115

[18] Suid M H, Ahmad M A (2021) Optimal tuning of sigmoid PID controller using Nonlinear Sine Cosine Algorithm for the Automatic Voltage Regulator system. ISA Transactions, 128(8): 265-286

[19] Eke I, Saka M, Gozde H, et al. (2021) Heuristic optimization based dynamic weighted state feedback approach for 2DOF PI-controller in automatic voltage regulator. Engineering Science and Technology an International Journal, 24(4): 899-910

[20] Micev M, Calasan M, Ali Z M, et al. Optimal design of automatic voltage regulation controller using hybrid simulated annealing -Manta ray foraging optimization algorithm. Ain Shams Engineering Journal, 12: 641-657

[21] Mohd-Tumari M Z, Ahmad M A, Suid M H, et al. (2023) An improved marine predators algorithm-tuned fractional-order PID controller for automatic voltage regulator system. Fractal Fract, 7(7): 1-38.

[22] Can O, Andic C, Ekinci S, et al. Enhancing transient response performance of automatic voltage regulator system by using a novel control design strategy. Electrical engineering, 2023(4): 105

[23] Ekinci S, Snášel V, Rizk-Allah RM, et al. (2024) Optimizing AVR system performance via a novel cascaded RPIDD2-FOPI controller and QWGBO approach, PLoS ONE, 19(5): e0299009

[24] Pathak P K, Yadav A K, Padmanaban S, et al. (2022) Fractional Cascade LFC for Distributed Energy Sources via Advanced Optimization Technique Under High Renewable Shares. IEEE Access, 10: 92828–92842

[25] Pathak P K, Yadav A K (2023) Design of optimal cascade control approach for LFM of interconnected power system. ISA Transactions, 137(6): 506-518

[26] Pathak P K, Yadav A K (2023) Fuzzy assisted optimal tilt control approach for LFC of renewable dominated micro-grid: A step towards grid decarbonization, Sustainable Energy Technologies Assessments, 60: 103551.1-103551.1360

[27] Ziegler J G, Nichols N B (1993) Optimum settings for automatic Controllers. Journal of Dynamic Systems Measurement and

Control, 64(2B): 759-768

[28] Cohen G H, Coon G A (1953) Theoretical consideration of retarded control. Journal of Fluids Engineering

[29] Ho W K, Hang C C, Cao L S (1992) Tuning of PI controllers based on gain and phase margin specifications. Proceedings of the IEEE International Symposium on Industrial Electronics, 2: 879-882

[30] Gaing Z L (2004) A particle swarm optimization approach for optimum design of PID controller in AVR system. IEEE Transactions on Energy Conversion, 19(2): 384-391

[31]Ekinci S, Izci D, Abu Zitar R, et al. (2022) Development of Lévy flight-based reptile search algorithm with local search ability for power systems engineering design problems. Neural Computing and Applications, 34(22): 20263-20283

[32] Izci D, Ekinci S (2022) An improved RUN optimizer based real PID plus second-order derivative controller design as a novel method to enhance transient response and robustness of an automatic voltage regulator. E-Prime - Advances in Electrical Engineering Electronics and Energy, 2: 100071.

[33] Pazhanimuthu C, Saravanan G, Suresh K (2023) Performance Analysis of Voltage Profile Improvement in AVR System using Zebra Optimization Algorithms based on PID Controller. E-Prime - Advances in Electrical Engineering, Electronics and Energy, 6: 100380

[34] Sikander A, Thakur P (2020) A new control design strategy for automatic voltage regulator in power system, ISA Transactions, 100(2B): 235-243

[35] Hekimoğlu B (2019) Sine-cosine algorithm-based optimization for automatic voltage regulator system. Transactions of the Institute of Measurement and Control, 41(6): 1761-1771.

[36]Ekinci S, Hekimoglu B (2019) Improved kidney-inspired algorithm approach for tuning of PID controller in AVR system. IEEE Access, 7: 39935-39947

[37] Rais M C, Dekhandji F Z, Recioui A, et al. (2022) Comparative study of optimization techniques based PID tuning for automatic voltage regulator system. Engineering Proceedings, 14(1): 21

[38] Kose E (2020) Optimal control of AVR system with tree seed algorithm-based PID controller. IEEE Access, 8: 89457-89467

[39] Saber A M, Behiry M H, Amin M (2022) Real-Time Optimization for an AVR System Using Enhanced Harris Hawk and IIoT, Studies in Informatics and Control, 31(2): 81-94

[40] Micev M, Ćalasan M, Oliva D (2021) Design and robustness analysis of an Automatic Voltage Regulator system controller by using Equilibrium Optimizer algorithm. Computers & Electrical Engineering, 89:106930

[41] Saravanan G, Suresh K P, Pazhanimuthu C (2024) Artificial rabbits optimization algorithm based tuning of PID controller parameters for improving voltage profile in AVR system using IoT, E-Prime - Advances in Electrical Engineering, Electronics and Energy, 8: 100523

[42] Mohd Tumari M Z, Ahmad M A, Mohd-Rashid M I, A fractional order PID tuning tool for automatic voltage regulator using marine predators algorithm, Energy Reports, 9(12): 416-421

[43] Tang Y, Cui M, Hua C, et al. (2012) Optimum design of fractional order PI λD μ controller for AVR system using chaotic ant swarm. Expert Systems with Applications, 39(8): 6887-6896

[44] Sikander A, Thakur P, Bansal R C, et al. (2017) A novel technique to design cuckoo search based FOPID controller for AVR in power systems. Computers & Electrical Engineering, 70: 261-274

[45] Khan I A, Alghamdi A S, Jumani T A, et al. (2019) Salp Swarm Optimization Algorithm-Based Fractional Order PID Controller for Dynamic Response and Stability Enhancement of an Automatic Voltage Regulator System. Electronics, 8(12): 1-17

[46] Altbawi S M A, Bin Mokhtar A S, Jumani T A, et al. (2024) Optimal design of Fractional order PID controller based Automatic voltage regulator system using gradient-based optimization algorithm. Journal of King Saud University - Engineering Sciences, 36(1): 32-44

[47] M. Karimi-Ghartemani, M. Zamani, N. Sadati, M. Parniani, An optimal fractional order controller for an AVR system using particle swarm optimization algorithm, LESCOPE'07-2007 Large Eng. Syst. Conf. Power Eng. (2007) 244–249. https://doi.org/10.1109/LESCPE.2007.4437386.

[47] Karimi-Ghartemani M, Zamani M, Sadati N, et al. (2007) An optimal fractional order controller for an AVR system using particle swarm optimization algorithm. Large Engineering Systems Conference on Power Engineering. 2007 in Montreal, Canada, pp: 244-249

[48] Verma B, Padhy P K (2020) Robust fine tuning of optimal PID controller with guaranteed robustness. IEEE Transactions on Industrial Electronics, 67(6): 4911-4920

[49] M.A. Ahmad, M.Z.M. Tumari, M.R. Ghazali, M.H. Suid, J.J. Jui, Robust PID tuning of AVR system based on Indirect Design Approach-2, in: 2023 Int. Conf. Syst. Sci. Eng., IEEE, 2023: pp. 522–526. https://doi.org/10.1109/ICSSE58758.2023.10227182.

[49] Ahmad M A, Tumari M Z M, Ghazali M R, et al. (2023) Robust PID tuning of AVR system based on Indirect Design Approach-2. International Conference on System Science and Engineering (ICSSE). 2023 in Ho Chi Minh, Vietnam, pp: 522-526

[50] Verma B, Padhy P K (2018) Optimal PID controller design with adjustable maximum sensitivity, IET Control Theory & Applications, 12(8): 1156-1165

[51] N. Mazibukol, K.T. Akindejil, G. Sharma, Implementation of a FUZZY logic controller (FLC) for improvement of an Automated Voltage Regulators (AVR) dynamic performance., 2022 IEEE PES/IAS PowerAfrica, PowerAfrica 2022. (2022) 4-8. https://doi.org/10.1109/PowerAfrica53997.2022.9905407.

Biographies

Mohd Zaidi Mohd Tumari received his first degree in B.Eng. Electrical Mechatronics and Master Degree in M.Eng Mechatronics and Automatic Control from University of Technology Malaysia (UTM) in 2008 and 2010, respectively. Currently, he is a Lecturer in Faculty of Electrical and Electronics Engineering Technology, Universiti Teknikal Malaysia Melaka (UTeM). His current research interests are model-free control, control of Mechatronic systems, nonlinear system identification and vibration control.

Mohd Ashraf Ahmad received his first degree in B.Eng Electrical Mechatronics and Master Degree in M.Eng Mechatronics and Automatic Control from University of Technology Malaysia (UTM) in 2006 and 2008, respectively. In 2015, he received a Ph.D in Informatics (Systems Science) from Kyoto University. Currently, he is an Associate Professor in the Faculty of Electrical and Electronics Engineering Technology, University Malaysia Pahang (UMP). His current research interests are model-free control, control of Mechatronic systems, nonlinear system identification and vibration control. He has been serving as Associate Editor for the International Journal of Electrical and Computer Engineering since 2016, Applications of Modelling and Simulation since 2017, and Journal of Future Robot Life since 2019.

Mohd Riduwan Ghazali received B-Eng. in Electrical-Mechatronics August 2007, M-Eng. in (Mechatronics & Automatic Control) at UTM Malaysia Mei 2010 and Doctor of Electronics Engineering, Universiti Malaysia Pahang, Malaysia December 2020. Currently Senior Lecturer at Universiti Malaysia Pahang, Malaysia. His research interest in data-driven control, mechatronics system, robotics and control instrumentations.

Mohd Helmi Suid received the B.Eng (Hons.) in Electrical and Electronics Engineering from Universiti Teknikal Melaka in 2007. In 2014, he receives M.Sc from School of Electronic and Electrical Engineering, University Sains Malaysia, Penang. He is currently, a lecturer in Faculty of Electrical and Electronics Engineering, University Malaysia Pahang (UMP). His current research interests are digital image processing, vision for robotics application and computational intelligence.

(Editor Zedong Zhang)